USER PARAMETER FREE APPROACHES TO MULTISTATIC ADAPTIVE ULTRASOUND IMAGING

Lin Du† Jian Li† Petre Stoica‡
†Dept. of Electrical and Computer Engineering, University of Florida, Gainesville, FL 32611-6130, USA.
‡Dept. of Information Technology, Uppsala University, SE-75105 Uppsala, Sweden.

ABSTRACT

Delay-and-sum (DAS) beamforming is the standard technique for ultrasound imaging applications. Due to its data independent property, DAS may suffer from poorer resolution and worse interference suppression capability than the adaptive standard Capon beamformer (SCB). However, the performance of SCB is sensitive to the errors in the sample covariance matrix and the signal steering vector. Therefore, robust adaptive beamforming techniques are desirable. In this paper, we consider ultrasound imaging via applying a user parameter free robust adaptive beamformer, which uses a shrinkage-based general linear combination (GLC) algorithm to obtain an enhanced estimate of the array covariance matrix. We present several multistatic adaptive ultrasound imaging (MAUI) approaches based on GLC to achieve high resolution and good interference suppression capability. The performance of the proposed MAUI approaches is demonstrated via an experimental example.

***Index Terms*— Adaptive beamforming, Ultrasound imaging**

I. INTRODUCTION

Delay-and-sum (DAS) beamforming is the standard technique for ultrasound imaging applications. Theoretically this data independent approach has lower resolution and worse interference suppression capability than an adaptive beamformer, e.g., the standard Capon beamformer (SCB) [1]. However, in practice, there is a clear performance degradation for SCB when the covariance matrix is inaccurately estimated due to limited data samples and when the knowledge of the steering vector is imprecise due to look direction errors or imperfect array calibration. Therefore, adaptive beamforming approaches that are robust to the aforementioned problems are desired.

Most of the early approaches to robust adaptive beamforming are ad-hoc techniques, e.g., the traditional diagonal loading algorithm [2], for which there is no clear way to choose the diagonal loading level. The diagonal loading algorithm has been previously applied to ultrasound imaging [3], where the diagonal loading level was set to be proportional to the received power. The robust Capon beamformer (RCB) presented in [4], on the other hand, can precisely calculate the diagonal loading level based on the uncertainty set of the steering vector. RCB was applied to ultrasound imaging in [5] and the results showed that RCB can provide much better imaging quality than DAS. However, we still need to specify the uncertainty set parameter for RCB, which may be hard to do in practice. To achieve user parameter free robust adaptive beamforming, we have recently devised several beamformers in [6] based on the shrinkage method, which can compute the diagonal loading level automatically without specifying any user parameters. Among these beamformers, the general linear combination (GLC) algorithm performs well, especially when the number of snapshots is small.

In this paper, we present several user parameter free approaches based on GLC for multistatic adaptive ultrasound imaging (MAUI), which form images of the backscattered energy for each focal point within the region of interest. All the MAUI approaches are two-stage imaging algorithms and GLC is employed in each stage. A similar idea can be applied to microwave imaging to replace the user parameter dependent RCB in each stage [7]. The complete multistatic data set for a given focal point can be represented by the data cube shown in Fig. 1. In one of the MAUI methods, which we refer to as MAUI-1, GLC is used in Stage I to obtain a set of backscattered signal estimates at each time instant. Based on these estimates, a scalar waveform is recovered via GLC in Stage II, which is then used to compute the backscattered energy. An alternative way of signal processing in Stage I is to compute a set of backscattered waveforms for each transmitter, which is referred to as MAUI-2. In addition, we also consider a combined method MAUI-C, which uses the signal estimates from both MAUI-1 and MAUI-2 in Stage I for the computation of backscattered energy. An experimental example will be presented to illustrate the performance of the MAUI methods.

Notation: The superscript $(\cdot)^*$ denotes the conjugate transpose, $(\cdot)^T$ denotes the transpose, $\lfloor x \rfloor$ denotes rounding to the greatest integer less than x, $E(\cdot)$ is the expectation operator, $\mathrm{tr}(\cdot)$ is the trace operator, and $\|\cdot\|$ denotes the Frobenius norm for a matrix or the Euclidean norm for a vector. Finally $\mathbf{R} \geq 0$ means that $\mathbf{R}$ is positive semi-definite.

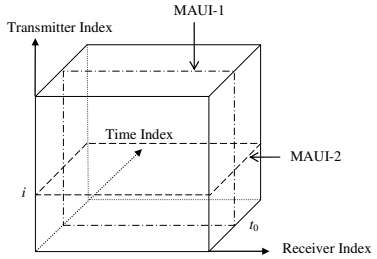

Fig. 1. The multistatic data cube. MAUI-1 processes the data set for a given time instant t_0, while MAUI-2 processes the data set for a given transmitter index i.

II. PROBLEM FORMULATION

Consider an active array of M transducers using the multistatic (also called MIMO (multi-input multi-output) [8]) data

The work was supported in part by the U.S. Army Medical Command under Grant No. W81XWH-06-1-0389, by the National Science Foundation under Grant No. CCF-0634786 and ECCS-0729727 and by the Swedish Research Council (VR).

acquisition scheme. Each transducer takes turns to transmit the same pulse while all of the transducers record the backscattered signals. As a result, the received data set $\{\mathbf{P}_{i,j}(t), \quad i,j=1,\cdots M; \quad t=0,\cdots,T-1\}$ comprises the A-scan data for all possible transmitter and receiver pairs of the array, where $\mathbf{P}_{i,j}(t)$ is the data sequence of the backscattered echo at the j^{th} transducer due to transmitting a pulse from the i^{th} transducer, and T is the number of data samples for the A-scan sequence.

To extend GLC to the wide-band ultrasound imaging application, we align the received signals from the data set $\{\mathbf{P}_{i,j}(t)\}$ to each focal point by inserting appropriate time delays. Let $\mathbf{r}_i$ and $\mathbf{r}_j$ denote the locations of the i^{th} transmitter and j^{th} receiver, respectively, and let $\mathbf{r}_f$ denote the location of a focal point in the imaging region of interest. The time delay due to the ultrasonic wave propagation from the i^{th} transmitter to the focal point $\mathbf{r}_f$ and then back to the j^{th} receiver is approximated as

$$\tau_{i,j}(\mathbf{r}_f) = \frac{1}{\Delta t}\left\lfloor \frac{\|\mathbf{r}_i - \mathbf{r}_f\|}{c} + \frac{\|\mathbf{r}_j - \mathbf{r}_f\|}{c} \right\rfloor, \tag{1}$$

where c is the sound propagation speed in the medium under interrogation, and Δt denotes the sampling interval. Then, the time shifted signal for a given focal point of interest $\mathbf{r}_f$ can be represented as

$$\begin{aligned} &y_{i,j}(\mathbf{r}_f,t) = \mathbf{P}_{i,j}(t+\tau_{i,j}(\mathbf{r}_f)),\\ &i,j=1,\cdots M; \quad t=0,\cdots,N-1, \end{aligned} \tag{2}$$

where N is determined by the duration of the transmitted pulse and the sampling interval Δt.

The problem of interest here is to form an ultrasound image on a grid of points in the imaging region. The image is formed from the received data set $\{\mathbf{P}_{i,j}(t)\}$, or more precisely, $\{y_{i,j}(\mathbf{r}_f,t)\}$, for each focal point of interest.

III. MAUI

The two-stage MAUI algorithms use a GLC-based robust adaptive beamforming algorithm in each stage. We first review the GLC approach and then we show how to apply GLC to the data set $\{y_{i,j}(\mathbf{r}_f,t)\}$ in Stages I and II of the proposed MAUI approaches.

A. *GLC*

In the GLC approach, we replace the sample covariance matrix in SCB by an enhanced estimate obtained via a shrinkage-based method. The enhanced covariance matrix estimate $\tilde{\mathbf{R}}$ is obtained by linearly combining the sample covariance matrix $\hat{\mathbf{R}}$ and a shrinkage target (we use the identity matrix $\mathbf{I}$ here for lack of a better choice) in an optimal mean-squared error (MSE) sense:

$$\tilde{\mathbf{R}} = \alpha\mathbf{I} + \beta\hat{\mathbf{R}}, \tag{3}$$

where $\hat{\mathbf{R}} = \frac{1}{K}\sum_{k=1}^{K}\mathbf{y}(k)\mathbf{y}^*(k)$, with the $L\times 1$ vector $\mathbf{y}(k)$ denoting the kth snapshot and K representing the total number of snapshots. The shrinkage parameters α and β in (3) are estimated by minimizing the MSE of $\tilde{\mathbf{R}}$ with respect to α and β, where

$$\begin{aligned} &\mathrm{MSE}(\tilde{\mathbf{R}}) = E\{\|\tilde{\mathbf{R}} - \mathbf{R}\|^2\}\\ &= \|\alpha\mathbf{I} - (1-\beta)\mathbf{R}\|^2 + \beta^2 E\{\|\hat{\mathbf{R}} - \mathbf{R}\|^2\}\\ &= \alpha^2 L - 2\alpha(1-\beta)\,\mathrm{tr}(\mathbf{R})\\ &+(1-\beta)^2\|\mathbf{R}\|^2 + \beta^2 E\{\|\hat{\mathbf{R}} - \mathbf{R}\|^2\},\\ &\mathbf{R} = E\left[\mathbf{y}(k)\mathbf{y}^*(k)\right]. \end{aligned} \tag{4}$$

The optimal values for β and α can be readily obtained:

$$\beta_0 = \frac{\gamma}{\rho+\gamma}, \tag{5}$$

$$\alpha_0 = \nu(1-\beta_0) = \nu\frac{\rho}{\gamma+\rho}, \tag{6}$$

where $\rho = E\{\|\hat{\mathbf{R}} - \mathbf{R}\|^2\}$, $\nu = \frac{\mathrm{tr}(\mathbf{R})}{L}$, and $\gamma = \|\nu\mathbf{I} - \mathbf{R}\|^2$. Note that $\beta_0 \in [0,1]$ and $\alpha_0 \geq 0$.

To estimate α_0 and β_0 from the given data, we need an estimate of ρ, which can be calculated as (see [9] for details):

$$\hat{\rho} = \frac{1}{K^2}\sum_{k=1}^{K}\|\mathbf{y}(k)\|^4 - \frac{1}{K}\|\hat{\mathbf{R}}\|^2. \tag{7}$$

Using (7) we can get estimates for β_0 and α_0 as

$$\hat{\beta}_0 = \frac{\hat{\gamma}}{\hat{\gamma}+\hat{\rho}}, \tag{8}$$

and

$$\hat{\alpha}_0 = \hat{\nu}(1-\hat{\beta}_0), \tag{9}$$

where $\hat{\nu} = \frac{\mathrm{tr}(\hat{\mathbf{R}})}{L}$, and $\hat{\gamma} = \|\hat{\nu}\mathbf{I} - \hat{\mathbf{R}}\|^2$. Note that $\hat{\alpha}_0 \geq 0$ and $\hat{\beta}_0 \geq 0$, which guarantees that the enhanced covariance matrix estimate $\tilde{\mathbf{R}} \geq 0$.

Substituting (8)-(9) in (3) yields the enhanced covariance matrix estimate $\tilde{\mathbf{R}}$. Using $\tilde{\mathbf{R}}$ instead of $\hat{\mathbf{R}}$ in the SCB formulation, we obtain the beamformer weight vector for GLC as follows:

$$\hat{\mathbf{w}} = \frac{\tilde{\mathbf{R}}^{-1}\bar{\mathbf{a}}}{\bar{\mathbf{a}}^*\tilde{\mathbf{R}}^{-1}\bar{\mathbf{a}}}, \tag{10}$$

where $\bar{\mathbf{a}}$ denotes the assumed steering vector [10]. Note that GLC is a diagonal loading approach with the diagonal loading level $\hat{\alpha}_0/\hat{\beta}_0$ determined automatically from the observed data snapshots $\{\mathbf{y}(k)\}_{k=1}^{K}$.

B. *Stage I*

To apply the GLC-based robust adaptive beamformer to the data set $\{y_{i,j}(\mathbf{r}_f,t)\}$ in (2), we use two approximate signal models for $y_{i,j}(\mathbf{r}_f,t)$ by making different assumptions. Since we will concentrate on the focal point $\mathbf{r}_f$ in what follows, the dependence on $\mathbf{r}_f$ will be dropped for notational simplicity.

The MAUI-1 algorithm uses the following signal model:

$$\mathbf{y}_i(t) = \mathbf{a}(t)s_i(t) + \mathbf{e}_i(t), \tag{11}$$

where $\mathbf{y}_i(t) = [y_{i,1}(t),\cdots,y_{i,M}(t)]^T$ represents the aligned array data vector of the i^{th} transmitter, $s_i(t)$ denotes the signal of interest (SOI) that is proportional to the ultrasound reflectivity or scattering strength, which is assumed to depend on the transmitter i but not on the receiver j, $\mathbf{e}_i(t)$ denotes the residual term due to noise and interferences, and $\mathbf{a}(t)$ denotes the array steering vector that is assumed to be approximately equal to $\mathbf{1}_{M\times 1}$. Here, we assume that $\mathbf{a}(t)$ may vary with t, but is constant with respect to the transmitter index i.

In Stage I, for a given time t_0, we form a pseudo-covariance matrix by considering the number of transmitters as the number of snapshots:

$$\hat{\mathbf{R}}(t_0) = \frac{1}{M}\mathbf{Y}(t_0)\mathbf{Y}^*(t_0),$$
$$\mathbf{Y}(t_0) = [\mathbf{y}_1(t_0)\cdots\mathbf{y}_M(t_0)]. \quad (12)$$

By using $\hat{\mathbf{R}}(t_0)$ as the sample covariance matrix we obtain an enhanced covariance matrix estimate $\tilde{\mathbf{R}}(t_0)$ as described in Section III.A, and then calculate the weight vector $\hat{\mathbf{w}}(t_0)$ for Stage I of MAUI-1 using (10) with $\bar{\mathbf{a}} = \mathbf{1}_{M\times 1}$ as:

$$\hat{\mathbf{w}}(t_0) = \frac{\tilde{\mathbf{R}}(t_0)^{-1}\bar{\mathbf{a}}}{\bar{\mathbf{a}}^*\tilde{\mathbf{R}}(t_0)^{-1}\bar{\mathbf{a}}}. \quad (13)$$

Once we got the weight vector, we can estimate $s_i(t_0)$ in (11) as:

$$\hat{s}_i(t_0) = \hat{\mathbf{w}}^*(t_0)\mathbf{y}_i(t_0). \quad (14)$$

Define a vector $\hat{\mathbf{s}}(t_0) = [\hat{s}_1(t_0),\cdots,\hat{s}_M(t_0)]^T$ of the estimated signals for all transmitters. Repeating the above process from $t_0 = 0$ to $t_0 = N-1$, we build the matrix $\hat{\mathbf{S}}_1 = [\hat{\mathbf{s}}(0),\cdots,\hat{\mathbf{s}}(N-1)]$.

The MAUI-2 algorithm considers another signal model:

$$\mathbf{y}_i(t) = \mathbf{a}_i s_i(t) + \mathbf{e}_i(t), \quad (15)$$

where $\mathbf{a}_i$ denotes the array steering vector, which is also assumed to be approximately equal to $\mathbf{1}_{M\times 1}$. However, different from MAUI-1, here $\mathbf{a}_i$ is assumed to change with i, but be constant with respect to t.

For a given transmitter i, the covariance matrix in Stage I of MAUI-2 is formulated as:

$$\hat{\mathbf{R}}_i = \frac{1}{N}\mathbf{Y}_i\mathbf{Y}_i^*,$$
$$\mathbf{Y}_i = [\mathbf{y}_i(0)\cdots\mathbf{y}_i(N-1)]. \quad (16)$$

Using $\hat{\mathbf{R}}_i$ as the sample covariance matrix we get an enhanced estimate $\tilde{\mathbf{R}}_i$, and then compute a weight vector $\hat{\mathbf{w}}_i$ using (10). The time sample vector of the corresponding beamformer output can be written as

$$\hat{\mathbf{s}}_i = [\hat{\mathbf{w}}_i^*\mathbf{Y}_i]^T. \quad (17)$$

Repeating the above process for $i = 1,\cdots,M$ yields a set of waveforms $\hat{\mathbf{S}}_2 = [\hat{\mathbf{s}}_1,\cdots,\hat{\mathbf{s}}_M]^T$.

As we mentioned before, the errors in the sample covariance matrix and the steering vector cause performance degradations for any adaptive beamforming algorithms. GLC is designed to improve the covariance matrix estimate. MAUI-1 and MAUI-2 use different sample covariance matrices. Hence the improvements obtained by using GLC may be different. This fact motivates us to combine MAUI-1 and MAUI-2 to achieve a better performance. We refer to this combined method, where $\hat{\mathbf{S}}_1$ of MAUI-1 and $\hat{\mathbf{S}}_2$ of MAUI-2 are used simultaneously, as MAUI-C. We denote the combined signal matrix as $\hat{\mathbf{S}}_C = \begin{bmatrix}\hat{\mathbf{S}}_1^T & \hat{\mathbf{S}}_2^T\end{bmatrix}^T$.

Let the $M \times 1$ vectors $\{\hat{\mathbf{s}}_m(t)\}_{t=0,\cdots,N-1}$ denote the columns of $\hat{\mathbf{S}}_m$ for $m = 1,2$, and let the $2M \times 1$ vectors $\{\hat{\mathbf{s}}_C(t)\}_{t=0,\cdots,N-1}$ denote the columns of $\hat{\mathbf{S}}_C$. Note that both MAUI-1 and MAUI-2 obtain M signal waveform estimates at the end of Stage I, while MAUI-C obtains $2M$ signal waveform estimates. We will apply GLC to these estimates in Stage II to recover a scalar waveform and compute the signal energy at the focal point.

C. *Stage II*

In Stage II, the signal model for both MAUI-1 and MAUI-2 can be represented as:

$$\hat{\mathbf{s}}_m(t) = \mathbf{a}_m s(t) + \mathbf{e}_m(t), \quad t = 0,\cdots,N-1, \quad m = 1,2, \quad (18)$$

where the steering vector $\mathbf{a}_m$ is assumed to be $\mathbf{1}_{M\times 1}$, and $\mathbf{e}_m(t)$ represents the residual term. Similar to Stage I, the knowledge of $\mathbf{a}_m$ may be imprecise and the sample size N may be small. Hence the GLC-based robust adaptive beamformer is used again to estimate $s(t)$. Taking $\hat{\mathbf{R}}_m$ as the sample covariance matrix:

$$\hat{\mathbf{R}}_m = \frac{1}{N}\sum_{t=0}^{N-1}\hat{\mathbf{s}}_m(t)\hat{\mathbf{s}}_m^*(t), \quad m = 1,2, \quad (19)$$

and paralleling the development in Stage I, we obtain the weight vector $\hat{\mathbf{w}}_m$ using (10). Then, the output signal estimate is computed as:

$$\hat{s}(t) = \hat{\mathbf{w}}_m^*\hat{\mathbf{s}}_m(t), \quad m = 1,2. \quad (20)$$

Finally, the signal energy for a particular focal point $\mathbf{r}_f$ is computed as:

$$\mathcal{E}(\mathbf{r}_f) = \sum_{t=0}^{N-1}\hat{s}^2(t). \quad (21)$$

For Stage II of MAUI-C, the signal model can be written as:

$$\hat{\mathbf{s}}_C(t) = \mathbf{a}_C s(t) + \mathbf{e}_C(t), \quad t = 0,\cdots,N-1, \quad (22)$$

where the vector $\hat{\mathbf{s}}_C(t)$ is considered now to be a snapshot from a $2M$-element "array", and the steering vector $\mathbf{a}_C$ is assumed to be $\mathbf{1}_{2M\times 1}$. $\mathbf{e}_C(t)$ denotes the residual term. We obtain the weight vector $\hat{\mathbf{w}}_C$ for MAUI-C via (10) by using the following sample covariance matrix:

$$\hat{\mathbf{R}}_C = \frac{1}{N}\sum_{t=0}^{N-1}\hat{\mathbf{s}}_C(t)\hat{\mathbf{s}}_C^*(t). \quad (23)$$

The beamformer $\hat{\mathbf{w}}_C$ yields an estimate of the signal:

$$\hat{s}(t) = \hat{\mathbf{w}}_C^*\hat{\mathbf{s}}_C(t). \quad (24)$$

Then, the backscattered energy at the focal point $\mathbf{r}_f$ is computed via (21).

IV. EXPERIMENTAL EXAMPLE

In this section, we present some experimental results to demonstrate the performance of the three MAUI algorithms. The complete multistatic data set was obtained by Bioacoustics Research Laboratory of the University of Illinois at Urbana-Champaign. The scene of interest contains several wire targets arranged in a complicated pattern. The data was collected using a 64-element linear array. The transducer center frequency was 2.6 MHz, the sampling rate was 25 MHz, and the sound velocity was assumed to be 1450 m/s. For comparison, the multistatic DAS scheme is also applied to the same data set. The DAS scheme estimates the signal waveform $s(t)$ as

$$\hat{s}(t) = \hat{\mathbf{w}}_{\text{DAS}}^*\mathbf{Y}(t)\hat{\mathbf{w}}_{\text{DAS}}, \quad t = 0,\cdots,N-1, \quad (25)$$

where $\hat{\mathbf{w}}_{\text{DAS}} = \bar{\mathbf{a}}/M$ is the weight vector for DAS. The backscattered energy at $\mathbf{r}_f$ is then estimated via (21).

Fig. 2 shows the ultrasound images for the wire data set under consideration. The images are displayed on a logarithmic scale with a 30 dB dynamic range. In Figs. 2 (a)-(d), we compare the images obtained via DAS and MAUI algorithms using only the central 32 elements of the array ($M = 32$). Since DAS simply sums all signals, the DAS image shown in Fig. 2 (a) has higher sidelobe level and poorer resolution than the MAUI images shown in Figs. 2 (b)-(d). Comparing Fig. 2 (b) and Fig. 2 (c), which correspond to MAUI-1 and MAUI-2 respectively, we note that MAUI-2 image has a lower background clutter level. However, MAUI-2 has poorer resolution: some wire targets are not discernable in the MAUI-2 image. On the other hand, the image obtained via MAUI-C has low sidelobe level similarly to MAUI-2 and high resolution similarly to MAUI-1. Moreover, all targets are clearly shown in the MAUI-C image. For comparison, we also include the DAS image obtained using the entire array ($M = 64$). Note that MAUI algorithms, especially MAUI-C, with 32 transducers can achieve similar imaging quality to DAS with a double sized array.

V. CONCLUSIONS

We have presented three user parameter free approaches to multistatic adaptive ultrasound imaging (MAUI). These two-stage MAUI approaches employ a GLC-based robust adaptive beamformer in each stage to achieve high resolution and good interference suppression capability, and also they are robust to small sample size problems and array steering vector errors. More importantly, GLC is a user parameter free approach as opposed to other existing robust adaptive beamforming algorithms, which makes it easy to use it in practice. The experimental results have demonstrated the effectiveness of the MAUI algorithms for ultrasound imaging. We have shown that the MAUI-C method, which combines MAUI-1 and MAUI-2, provides the best imaging quality.

REFERENCES

[1] J. Capon, "High resolution frequency-wavenumber spectrum analysis," *Proceedings of the IEEE*, vol. 57, pp. 1408–1418, August 1969.

[2] H. Cox, R. Zeskind, and M. Owen, "Robust adaptive beamforming," *Proceedings of IEEE*, vol. ASSP-35, pp. 1365–1375, October 1987.

[3] J. Synnevåg, A. Austeng, and S. Holm, "Adaptive beamforming applied to medical ultrasound imaging," *IEEE Transactions on Ultrasonics, Ferroelectrics, and Frequency Control*, vol. 54, no. 8, pp. 1606–1613, 2007.

[4] J. Li, P. Stoica, and Z. Wang, "On robust Capon beamforming and diagonal loading," *IEEE Transactions on Signal Processing*, vol. 51, pp. 1702–1715, July 2003.

[5] Z. Wang, J. Li, and R. Wu, "Time-delay and time-reversal based robust Capon beamformers for ultrasound imaging," *IEEE Transactions on Medical Imaging*, vol. 24, no. 10, pp. 1308–1322, 2005.

[6] J. Li, L. Du, and P. Stoica, "Fully automatic computation of diagonal loading levels for robust adaptive beamforming," submitted to *IEEE Transactions on Aerospace and Electronic Systems*, 2007.

[7] Y. Xie, B. Guo, J. Li, and P. Stoica, "Novel multistatic adaptive microwave imaging methods for early breast cancer detection," *EURASIP Journal on Applied Signal Processing*, vol. 2006, pp. 1–12, 2006.

[8] J. Li and P. Stoica, "MIMO radar with colocated antennas: Review of some recent work," *IEEE Signal Processing Magazine*, vol. 24, no. 5, pp. 106–114, 2007.

[9] P. Stoica, J. Li, X. Zhu, and J. R. Guerci, "On using a priori knowledge in space-time adaptive processing," to appear in *IEEE Transactions on Signal Processing*, 2007.

[10] P. Stoica and R. L. Moses, *Spectral Analysis of Signals*. Upper Saddle River, NJ: Prentice-Hall, 2005.

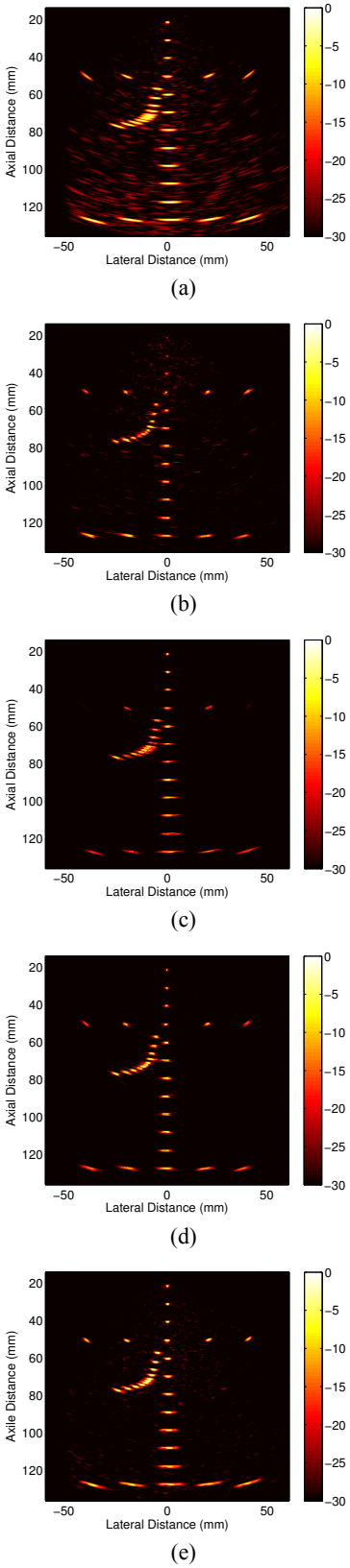

Fig. 2. Ultrasound images obtained via (a) DAS with $M = 32$, (b) MAUI-1 with $M = 32$, (c) MAUI-2 with $M = 32$, (d) MAUI-C with $M = 32$, and (e) DAS with $M = 64$.